

THE SCHWERDTFEGER LIBRARY
1225 W. Dayton Street
Madison, WI 53706

RELATIVE IMPROVEMENTS IN VAS
CALIBRATION USING A HEATED
INTERNAL BLACKBODY

By .

L.A. Sromovsky

20 September 1974

University of Wisconsin
Space Science and Engineering Center
1225 West Dayton Street
Madison, Wisconsin 53706

TABLE OF CONTENTS

1. INTRODUCTION	1
2. Radiative Model of the VAS Telescope	2
3. A Lumped Description of the VAS Instrument	5
4. Two Approaches to VAS Calibration	8
5. Relative Sensitivities to Errors	10
6. Combined Effects of Random Errors	13
7. Effects of Systematic Errors	14

1. INTRODUCTION

In a previous analysis (Sromovsky, 1974) it was found that VAS calibration accuracy could be improved by providing an auxiliary space view which by passed the primary telescope. Compared to the original VAS calibration using an internal ambient blackbody the additional measurement resulted in significantly reduced sensitivity to bias errors induced by systematic errors in laboratory measurements and possible in-orbit degradation of optical components.

However, serious difficulties in the implementation of the auxiliary space view appear to make it impractical. An alternative technique which can, in principal, achieve the same objective as the auxiliary space view is to provide two internal radiation references at different levels. The specific implementation of this approach now being considered is to provide the VAS internal blackbody with a heater so that it can be operated at two significantly different temperatures. Formally this should provide the same information as the internal space view. The analysis presented here provides quantitative error estimates for this new approach compared to the original VAS calibration procedure.

It should be noted that the present VAS calibration analysis also includes two new factors which have been previously neglected, i.e. emission from the primary and secondary mirror masks which can enter the relay exit pupil. As a result the radiometric model of the VAS primary telescope has been slightly modified.

2. Radiative Model of the VAS Telescope

Radiation entering the relay exit pupil during external target measurements is a weighted average of radiation from the target (alternated by the telescope) and radiation from optical components. If N_T is the radiance of the target and $B(T_i)$ is the blackbody radiance of the i^{th} optical component within the relay exit pupil, then the average radiance within the relay exit pupil can be expressed as

$$N_E = \tau N_T + \sum_{i=1}^7 a_i B(T_i) \quad (1)$$

where

$$\tau = 1 - \sum_{i=1}^7 a_i \quad (2)$$

$B(T_i)$ = Planck radiance at temperature T_i , and where, the seven effective emissivity coefficients a_i and the corresponding component temperatures T_i are identified in Table 1. A schematic diagram of the VAS telescope is presented in Figure 1.

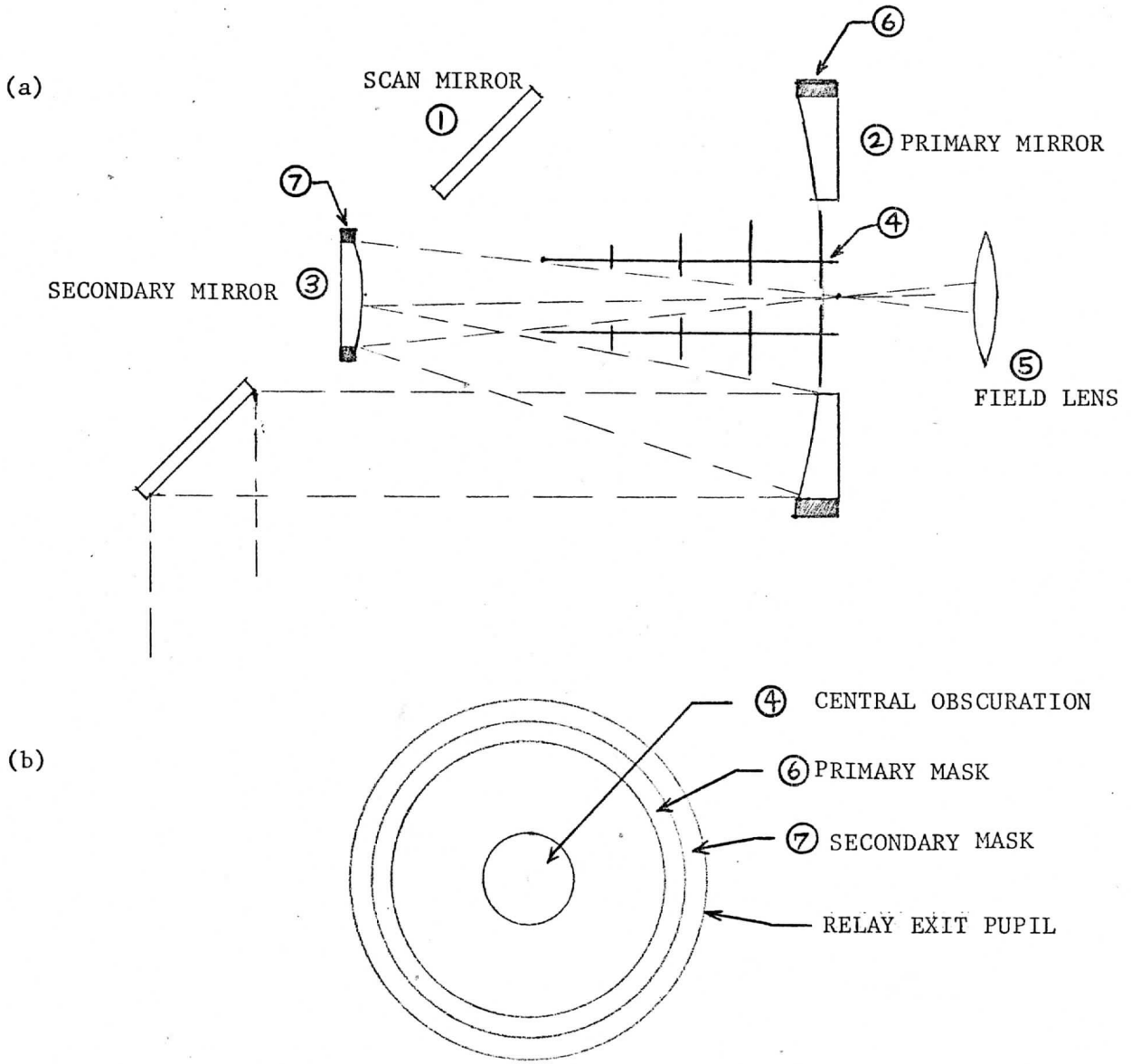


FIGURE 1. SCHEMATIC DIAGRAM OF VAS TELESCOPE (a) AND OBSCURATIONS WITHIN THE RELAY SYSTEM FIELD OF VIEW (b)

TABLE 1. Components of the VAS Telescope Radiative Model

<u>i</u>	<u>COMPONENT NAME</u>	<u>TEMPERATURE</u>	<u>a_i</u>
1	scan mirror	T ₁	(1-R ₁)R ₂ R ₃ τ _f (1-K ₄ -K ₆ -K ₇)
2	primary mirror	T ₂	(1-R ₂)R ₃ τ _f (1-K ₄ -K ₆ -K ₇)
3	secondary mirror	T ₃	(1-R ₃)τ _f (1-K ₇)
4	central obscuration	T ₄	K ₄ R ₃ τ _f
5	field lens	T ₅	1-τ _f
6.	primary mask	T ₆	K ₆ •R ₃ •τ _f
7.	secondary mask	T ₇	K ₇ τ _f

Parameters used to describe the a_i coefficients are defined below (see Figure 1).

R₁, R₂, R₃ = reflectivities of the scan mirror, primary mirror, and secondary mirror respectively

τ_f = transmission of the field lens

K₄ = ratio of the central obscuration solid angle to the exit pupil solid angle

K₆ = fraction of the exit pupil solid angle obscured by the primary mirror mask

K₇ = fractional solid angle obscured by the secondary mirror mask

Nominal values assumed for these fundamental optical constants are:

$$\left. \begin{aligned}
 R_1=R_2=R_3 &= 0.96, \\
 \tau_f &= 0.90, \\
 K_4 &= 0.131, \\
 K_6 &= 0.060, \text{ and} \\
 K_7 &= 0.121.
 \end{aligned} \right\}$$

(3)

The total fractional obscuration is thus

$$K_4 + K_6 + K_7 = 0.312, \quad (4)$$

and the net telescope transmission is

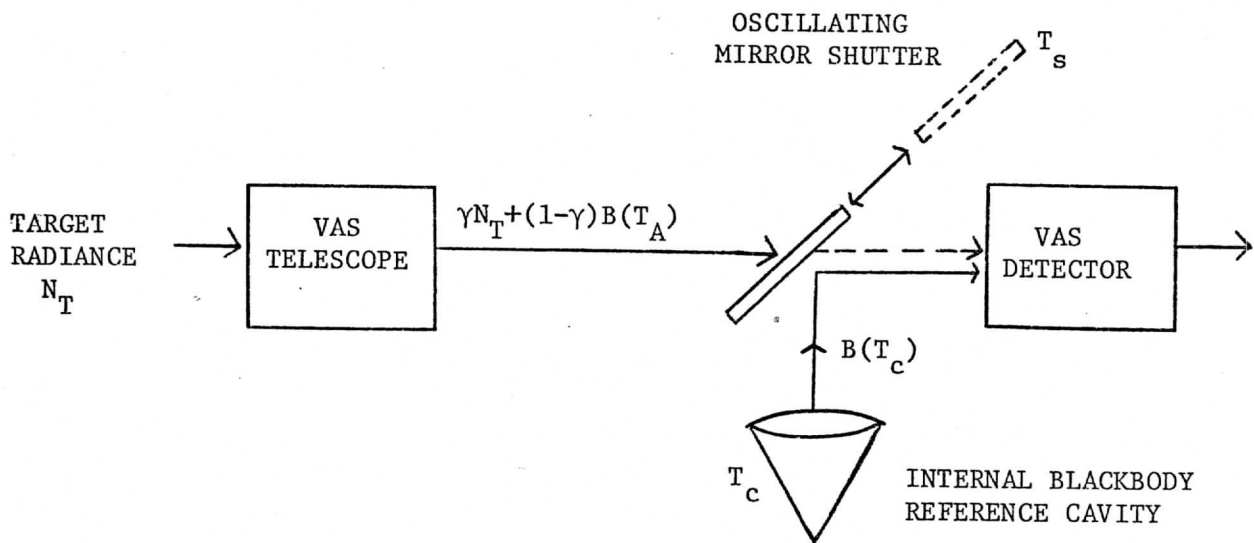
$$\tau = R_1 R_2 R_3 \tau_f (1 - K_4 - K_6 - K_7) = 0.5478. \quad (5)$$

3. A Lumped Description of the VAS Instrument

A condensed description of the VAS and its radiation sources and targets is presented in Figure 2. In the original VAS design the internal blackbody operated at only one temperature, the ambient temperature of the VAS aft optics cavity. In the case of the heated blackbody presently under consideration T_c will be allowed to assume two distinct values.

There are three qualitatively different measurements which must be considered in the VAS calibration. These are defined below.

<u>VIEW</u>	<u>SIGNAL OUTPUT</u>
space through VAS telescope	$V_1 = \alpha (1-\tau)B(T_A) + V_o \quad (6)$
internal blackbody reference cavity	$V_2 = \alpha [R_s B(T_c) + (1-R_s)B(T_s)] + V_o \quad (7)$
external target	$V_4 = \alpha [\epsilon N_T + (1-\tau)B(T_A)] + V_o \quad (8)$



- TARGET = Space, earth, or equivalent external blackbody.
- VAS TELESCOPE = Scan mirror, primary telescope, and field lens.
- VAS DETECTOR = Relay optics (excluding field lens), detectors, and electronics. Final output is a voltage signal V .
- INTERNAL BLACKBODY = High emissivity cone at a known temperature T_c used to insert a known radiation level into the VAS detector.
- OSCILLATING MIRROR SHUTTER = A gold mirror which oscillates in and out of the optical path providing alternate views through the VAS telescope and into the reference cavity

FIGURE 2. LUMPED DESCRIPTION OF THE VAS RADIOMETER

The parameters used in expressions for the VAS signal output are defined as follows:

- α = responsivity of the VAS detector system (volts/unit radiance).
- τ = transmission of the VAS telescope (equation 21).
- T_A = weighted average temperature of the VAS telescope.
- T_S = temperature of the mirror shutter.
- T_C = temperature of the internal blackbody cavity.
- R_S = reflectivity of the mirror shutter.
- $B(T)$ = Planck spectral radiance of a blackbody at temperature T (dependence on wavelength is implicit).

The weighting used to obtain T_A is defined by the condition

$$(1-\tau) B(T_A) = \sum_{i=1}^7 a_i B(T_i). \quad (9)$$

The basic calibration equation relating target radiance to line-by-line voltage measurements (voltages measured for every scan line) is just

$$N_T = B(T^*) (V_4 - V_1) / (V_2 - V_1), \quad (10)$$

where, in this case, V_2 is measured for T_C at ambient. The formal expression for $B(T^*)$, the radiance of an external blackbody at temperature T^* which would produce the same response as the internal blackbody at temperature T_C , is obtained from equations (6) through (8), i.e.

$$B(T^*) = \frac{1}{\tau} [(1-\tau)B(T_A) + R_S B(T_C) + (1-R_S)B(T_S)]. \quad (11)$$

However, since this quantity is only used while the cavity is at ambient temperature T_L we are able to simplify this expression to the form

$$B(T^*) = \frac{1}{\tau} [(1-\tau)B(T_A) + B(T_L)], \quad (12)$$

where we have justifiably assumed that

$$T_s = (T_c)_{\text{ambient}} \equiv T_L. \quad (13)$$

In the subsequent analysis only the $B(T^*)$ term of equation (10) will be considered in estimating calibration errors (the voltage factors have errors which are more properly described as measurement errors). Furthermore, equation (12) will be used exclusively to define $B(T^*)$.

4. Two Approaches to VAS Calibration

In general we must consider two different sets of calibration measurements taken at different times and at different blackbody cavity temperatures. In both the ambient blackbody and the heated blackbody cases there are calibration measurements made during every scan line while the cavity is at ambient temperature. In the case of the heated cavity there is another set of measurements made at a different time with the cavity heated to some higher temperature T_H in addition to first operating at temperature T_L . The first set of measurements are obviously made very frequently, while the second set is made only occasionally. Thus the second set can in general be affected by different parameter values than the first. Both sets are defined below.

<u>TIME STATUS</u>	<u>VIEW</u>	<u>SIGNAL OUTPUT</u>	
CURRENT (LINE-BY-LINE)	$\left\{ \begin{array}{l} \text{SPACE} \\ \text{CAVITY} \end{array} \right.$	$V_1 = \alpha(1-\tau)B(T_A) + V_O$	(14)
		$V_2 = \alpha B(T_L) + V_O$	(15)
OCCASIONAL	$\left\{ \begin{array}{l} \text{SPACE} \\ \text{AMBIENT CAVITY} \\ \text{HEATED CAVITY} \end{array} \right.$	$V_1' = \alpha' (1-\tau')B(T_A') + V_O'$	(16)
		$V_2' = \alpha' B(T_L') + V_O'$	(17)
		$V_3' = \alpha' [R_S B(T_H') + (1-R_S)B(T_S')] + V_O'$	(18)

For METHOD 1 (ambient blackbody) only current measurements are available, i.e. V_1 , V_2 and component temperatures. Estimated quantities are a_i , $i = 1, 7$ and $\tau = 1 - \sum_{i=1}^7 a_i$. The solution for $B(T^*)$ is found using equation (12) and the estimated quantities, i.e.

$$\text{METHOD 1: } B(T_1^*) = \frac{1}{\tau} [B(T_L) - (1-\tau)B(T_A)] \quad (19)$$

where $B(T_A)$ is given by equation (9) in terms of the a_i and T_i . The subscript on T_1^* is used to denote the T^* value derived by Method 1. $B(T_1^*)$, V_1 and V_2 are then inserted in equation (10).

For METHOD 2 (heated blackbody) both current and occasional measurements are used. The occasional measurements are used to derive an improved estimate of τ' which has the formal solution

$$\tau' = 1 - \frac{B(T_L')}{B(T_A')} + \frac{(V_2' - V_1')}{(V_2' - V_3')} \cdot \frac{B(T_L') - R_S B(T_H') - (1 - R_S)B(T_S')}{B(T_A')} \quad (20)$$

Since a_i , $i = 1, 7$ and R_S are theoretical estimates in practice and $B(T_A')$ is an estimate based on the a_i and measured temperature values, the derived value of τ' using equation (20) is, in general, different from the exact value, it is desirable to define a new parameter γ :

$$\text{METHOD 2: } \gamma \equiv (\tau')_{\text{ESTIMATED USING EQ. 20}} \quad (21)$$

The parameter γ is used in equation (19) in place of τ to obtain T_2^* , i.e.

$$\text{METHOD 2: } B(T_2^*) = \frac{1}{\gamma} [B(T_L) - (1-\gamma)B(T_A)], \quad (22)$$

where we have used the notation

$$B(T_A') = \sum_{i=1}^7 a_i' B(T_i'), \text{ and} \quad (23)$$

$$B(T_A) = \sum_{i=1}^7 a_i B(T_i). \quad (24)$$

It should be noted that although we allow the case $\alpha' \neq \alpha$, it is assumed that $a'_i = a_i$ and consequently that $\tau' = \tau$. Cases for which $a'_i \neq a_i$ are not dealt with in this analysis.

5. Relative Sensitivities to Errors

In determining T_1^* and T_2^* a large number of parameters must be either estimated or measured. A complete list is provided below:

ESTIMATED OPTICAL CONSTANTS	$R_1, R_2, R_3, \tau_f, K_4, K_6, K_7, R_s$
OCCASIONAL TEMPERATURE MEASUREMENTS	$T'_L, T'_H, T'_S, T'_i, i=1,7$
CURRENT TEMPERATURE MEASUREMENTS	$T_L, T_i, i=1,7$
OCCASIONAL VOLTAGE MEASUREMENTS	V'_1, V'_2, V'_3

Since all of these parameters will contain errors there will also be errors in T_1^* and T_2^* . If x_k denotes the k^{th} parameter of the 29 just tabulated then the error in T_1^* or T_2^* can be obtained from the following expressions

$$\text{SYSTEMATIC ERROR} \quad \delta T_{1,2}^* = \sum_{k=1}^{29} \frac{\partial T_{1,2}^*}{\partial x_k} \delta x_k \quad (25)$$

$$\text{RANDOM ERROR} \quad \sigma_{T_{1,2}^*} = \left[\sum_{k=1}^{29} \left(\frac{\partial T_{1,2}^*}{\partial x_k} \right)^2 \sigma_{x_k}^2 \right]^{1/2} \quad (26)$$

where δx_k and σ_{x_k} are systematic and random errors respectively in the parameter x_k .

The partial derivatives have been numerically evaluated for METHOD 1 using equation (19) and for METHOD 2 using equations (20), (21) and (22). Results for both methods are presented in Table 2. These results are valid for the following specific conditions

$R_s = 0.96$	$T'_H = 340^\circ\text{K}$	(27)
	$T'_S = 300^\circ\text{K}$	
$T_L = 300^\circ\text{K}$	$T'_L = 300^\circ\text{K}$	
$T_L - T_1 = 3.34^\circ\text{K}$	$T'_L - T'_1 = 3.34^\circ\text{K}$	
$T_L - T_2 = 2.16^\circ\text{K}$	$T'_L - T'_2 = 2.16^\circ\text{K}$	
$T_L - T_3 = 8.54^\circ\text{K}$	$T'_L - T'_3 = 8.54^\circ\text{K}$	
$T_L - T_4 = 6.47^\circ\text{K}$	$T'_L - T'_4 = 6.47^\circ\text{K}$	
$T_L - T_5 = 2.16^\circ\text{K}$	$T'_L - T'_5 = 2.16^\circ\text{K}$	
$T_L - T_6 = 2.16^\circ\text{K}$	$T'_L - T'_6 = 2.16^\circ\text{K}$	
$T_L - T_7 = 8.54^\circ\text{K}$	$T'_L - T'_7 = 8.54^\circ\text{K}$	
$\alpha = 0.024 \text{ V}/(\text{erg}/\text{etc.})$	$\alpha' = 0.012 \text{ V}/(\text{erg}/\text{etc.})$	

The temperature gradients are based on VISSR thermal model calculations for day 172 (a worst case condition). An additional implicit parameter is the wave number ν . Although results in Table 2 apply for $\nu = 680 \text{ cm}^{-1}$, the temperature equivalent errors will not change significantly for other VAS spectral intervals.

Comparing results for T_2^* with those for T_1^* we find that T_2^* is significantly less sensitive to optical constant uncertainties on the average and slightly more sensitive to temperature measurement errors as a result of the greater number of temperature measurements required. Note that errors in the unprimed temperatures are much more significant than errors in the primed temperatures.

Table 2. T* Derivatives for METHODS 1 and 2 with Respect to Parameters used in Calibration

<u>k</u>	<u>x_k</u>	$\frac{\partial T_1^*}{\partial x_k}$	$\frac{\partial T_2^*}{\partial x_k}$
1	R ₁	- 7.67°K	+ 2.16°K
2	R ₂	- 6.45°K	+ 3.56°K
3	R ₃	-14.25°K	- 5.33°K
4	τ _f	- 4.22°K	+ 6.83°K
5	K ₄	+15.70°K	+ 2.33°K
6	K ₆	+ 9.15°K	- 4.85°K
7	K ₇	+18.80°K	+ 5.73°K
8	R _s	-	+10.64°K
9	T _L	1.79	1.79
10	T ₁	- 0.040	- 0.040
11	T ₂	- 0.042	- 0.042
12	T ₃	- 0.054	- 0.054
13	T ₄	- 0.196	- 0.196
14	T ₅	- 0.177	- 0.177
15	T ₆	- 0.092	- 0.092
16	T ₇	- 0.186	- 0.186
17	T _H	-	- 0.28
18	T _s	-	- 0.01
19	T _L	-	+ 0.45
20	T ₁	-	- 0.005
21	T ₂	-	- 0.005
22	T ₃	-	- 0.006
23	T ₄	-	- 0.022

Table 2. Continued

k	x_k	$\frac{\partial T_1^*}{\partial x_k}$	$\frac{\partial T_2^*}{\partial x_k}$
24	T_5'	-	- 0.020
25	T_6'	-	- 0.011
26	T_7'	-	- 0.021
27	V_1'	-	+10.05°K/V
28	V_2'	-	-22.12°K/V
29	V_3'	-	+12.12°K/V

6. Combined Effects of Random Errors

The effect of randomly distributed parameter uncertainties on T^* errors can be calculated using equation (26) and the derivatives listed in Table 2. Although there are 29 parameters to be considered there are only three different standard deviations associated with three different parameter groups: optical constants, temperature measurements, and voltage measurements. These are defined as follows:

$$\sigma_R \equiv \sigma_{R_1} = \sigma_{R_2} = \sigma_{R_3} = \sigma_T = \sigma_{K_4} = \sigma_{k_6} = \sigma_{K_7} = \sigma_{R_s} \quad (28)$$

$$\sigma_T \equiv \sigma_{T_L} = \sigma_{T_L'} = \sigma_{T_S'} = \sigma_{T_H'} = \sigma_{T_{i,i=1,7}} = \sigma_{T_{i,i=1,7}'} \quad (29)$$

$$\sigma_V \equiv \sigma_{V_1'} = \sigma_{V_2'} = \sigma_{V_3'} \quad (30)$$

Equation (26) can then be written in the two forms

$$\sigma_{T_1^*} = \left[\sum_{k=1}^7 \left(\frac{\partial T_1^*}{\partial x_k} \right)^2 \sigma_R^2 + \sum_{k=9}^{16} \left(\frac{\partial T_1^*}{\partial x_k} \right)^2 \sigma_T^2 \right]^{1/2} \quad (31)$$

$$\sigma_{T_2}^* = \left[\sum_{k=1}^8 \left(\frac{\partial T_2^*}{\partial x_k} \right)^2 \sigma_R^2 + \sum_{k=9}^{26} \left(\frac{\partial T_2^*}{\partial x_k} \right)^2 \sigma_T^2 + \sum_{k=27}^{28} \left(\frac{\partial T_2^*}{\partial x_k} \right)^2 \sigma_V^2 \right]^{1/2}. \quad (32)$$

Inserting derivative values from Table 2 yields the following numerical results:

$$\sigma_{T_1}^* = [1000.5(^{\circ}\text{K})^2 \sigma_R^2 + 3.324 \sigma_{T_2}^2]^{1/2} \quad (33)$$

$$\sigma_{T_2}^* = [267.4(^{\circ}\text{K})^2 \sigma_R^2 + 3.606 \sigma_T^2 + 737.2 \left(\frac{^{\circ}\text{K}}{\text{V}} \right)^2 \sigma_V^2]^{1/2} \quad (34)$$

If we assume an RMS voltage error equal to the RMS 8-bit quantizing error of $5 \times 10^{-3}\text{V}$ and the SBRC estimates of

$$\left. \begin{aligned} \sigma_R &= .01 \\ \sigma_T &= 0.13^{\circ}\text{K}, \end{aligned} \right\} \quad (35)$$

then the T^* standard deviations expressed by equations (33) and (34) take on the specific values

$$\left. \begin{aligned} \sigma_{T_1}^* &= 0.395^{\circ}\text{K} \\ \sigma_{T_2}^* &= 0.326^{\circ}\text{K}. \end{aligned} \right\} \quad (36)$$

Thus we see that both methods have substantially the same performance under the assumed conditions of randomly distributed errors and Day 172 temperature gradients, although $\sigma_{T_2}^*$ is slightly smaller and T_2^* is much less sensitive than T_1^* to optical parameter errors.

7. Effects of Systematic Errors

The systematic T^* errors δT_1^* and δT_2^* can be computed using equation (25), the derivatives in Table 2, and estimated systematic parameter errors δx_k . First let us consider the case of uniform systematic error, i.e.

$$\left. \begin{aligned} \delta R_1 = \delta R_2 = \delta R_3 = \delta \tau = \delta R_s &\equiv \delta R \\ \delta K_4 = \delta K_6 = \delta K_7 &\equiv 0 \\ \delta T &= 0 \end{aligned} \right\} \quad (37)$$

In this case we find, for Day 172 temperatures, the specific results

$$\left. \begin{aligned} \delta T_1^* &= (-32.6^\circ\text{K}) \delta R \\ \delta T_2^* &= (+17.9^\circ\text{K}) \delta R. \end{aligned} \right\} \quad (38)$$

Specific values of δR and resulting T^* errors are presented in Table 3 for two cases of interest.

Table 3. Examples of T^* Bias Errors Resulting from Uniform Systematic Optical Constant Errors

δR	δT_1^*	δT_2^*
± 0.005 (systematic error in laboratory measurements)	$\pm 0.16^\circ\text{K}$	$\pm 0.09^\circ\text{K}$
$- 0.03$ (possible in-orbit degradation of optical components)	$+ 0.98^\circ\text{K}$	$- 0.54^\circ\text{K}$

The major cause for the relatively small improvement of METHOD 2 over METHOD 1 is the high sensitivity of T_2^* to errors in the shutter mirror reflectivity R_3 (see Table 2). This effect can also be seen in Tables 4 and 5 which present cases on nonuniform degradation.

For the case of nonuniform systematic errors results vary considerably with the distribution of errors among optical components. In Table 4 results are presented for many cases in which fixed transmission loss of 20% is assumed. For simplicity, when more than one optical component degrades, all are assumed to degrade the same amount. Note that METHOD 2 has a strong

advantage over METHOD 1 except when R_s is degraded.

Another way to compare in-orbit degradation effects is to assume a fixed degradation per element and determine T* errors as different combinations of elements are allowed to degrade. Results for a fixed degradation of 0.05 are presented in Table 5. Again, we find that METHOD 2 is much better than METHOD 1 only when R_s is not degraded. A summary of all the cases presented in both Tables is presented in Table 6.

Although the magnitude of the per element degradations assumed for the examples of Tables 4 and 5 are probably much larger than is likely to be found in-orbit, it does allow relative comparisons of the two methods. However, the absolute comparison becomes very significant in deciding whether or not to implement the second, more complicated method. Better estimates of likely in-orbit degradation and evaluation of errors for more representative temperature gradients than just the extreme Day 172 case.

Table 4. T* Bias Errors for a 20% Transmission Loss as a Function of which Elements are Degraded

Parameters which are degraded equally to yield a net 20% drop in transmission

	<u>Individual Parameter Change</u>	<u>δT_1^*</u>	<u>δT_2^*</u>
R_1 (scan mirror)	-.192	+1.47°K	-0.41°K
R_1, R_2	-.101	+1.43°K	-0.58°K
R_1, R_3	-.101	+2.21°K	+0.32°K
R_1, R_2, R_3	-.069	+1.96°K	-0.03°K
τ_f	-.180	+0.76°K	-1.23°K
R_1, R_3, τ_f	-.068	+1.78°K	-0.25°K
R_1, R_2, R_3, τ_f	-.052	+1.69°K	-0.38°K
R_s, R_1	-.192	-	-2.46°K
R_s, R_1, R_2	-.101	-	-1.65°K
R_s, R_1, R_2, R_3	-.069	-	-0.76°K
R_s, τ_f	-.180	-	-3.15°K
R_s, R_1, R_3, τ_f	-.068	-	-0.97°K
$R_s, R_1, R_2, R_3, \tau_f$	-.052	-	-0.93°K

Table 5. T* Bias Errors Resulting from 0.05 Regradation per Element as a Function of the Combination of Elements which Degrade

<u>Parameters which Degrade</u>	<u>δT_1^*</u>	<u>δT_2^*</u>	<u>Net Transmission Loss</u>
R_1	+ .38°K	-0.11°K	5.2%
R_1, R_2	+ .76°K	-0.29°K	10.1%
R_1, R_3	+1.10°K	+0.16°K	10.1%
R_1, R_2, R_3	+1.42°K	-0.02°K	14.8%
τ_f	+0.21°K	-0.34°K	5.6%
R_1, R_3, τ_f	+1.31°K	-0.18°K	15.1%
R_1, R_2, R_3, τ_f	+1.63°K	-0.36°K	19.6%
R_s, R_1	-	-0.64°K	5.2%
R_s, R_1, R_2	-	-0.82°K	10.1%
R_s, R_1, R_3	-	-0.37°K	10.1%
R_s, R_1, R_2, R_3	-	-0.55°K	14.8%
R_s, τ_f	-	-0.87°K	5.6%
R_s, R_1, R_3, τ_f	-	-0.71°K	15.1%
$R_s, R_1, R_2, R_3, \tau_f$	-	-0.89°K	19.6%

Table 6. Summary of Results for all Degradation Cases
Considered in Tables 3 and 4

	<u>METHOD 1</u> <u>(AMBIENT BLACKBODY)</u>	<u>METHOD 2</u> <u>(HEATED BLACKBODY)</u>
Bias error averaged over all cases	+1.29°K	-0.68°K
Bias error absolute value averaged over all cases	1.29°K	0.72°K
% cases exceeding 1.5°K absolute error	36%	11%
% cases exceeding 1.0°K absolute error	71%	15%
% cases exceeding 0.5°K absolute error	86%	52%